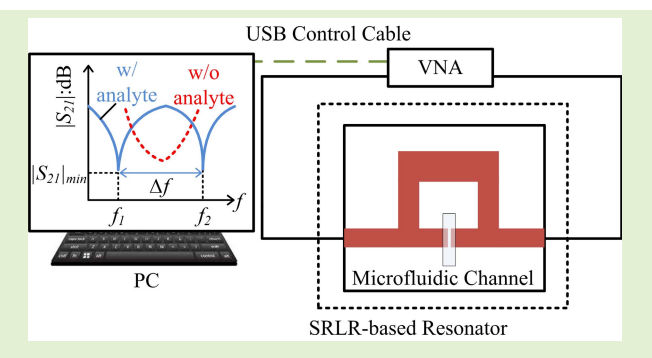


# A Dual-Mode Microwave Resonator for Liquid Chromatography Applications

Duye Ye<sup>®</sup>, Omkar, and Pingshan Wang<sup>®</sup>, Senior Member, IEEE

Abstract—This work presents a microwave microfluidic sensor for high performance liquid chromatography (HPLC) applications. The sensor is based on a modified square ring loaded resonator (SRLR), where a transmission line and a ring are electrically shorted with a center gap. A microfluidic channel is bonded above the gap for liquid-under-test (LUT) measurement. When the dielectric constant of LUT is above a threshold value, two degeneration modes of the resonator are separated, resulting in two transmission-zero frequencies. The threshold dielectric constant can be easily tuned by the gap size. High sensitivity is achieved when LUT dielectric constant is close to the threshold value. These features enable the proposed resonator to be optimized for different microfluidic



applications. To validate the design, three resonators with 10  $\mu$ m, 30  $\mu$ m and 90  $\mu$ m gap sizes are built and tested with water-methanol solutions in various volume fractions. Additionally, the sensor is connected in series with HPLC system for caffeine and sucrose detection. The detection linearity is characterized by measuring water-caffeine samples from 0.77 ppm to 1000 ppm. A 0.231 ppm limit of detection (LOD) is achieved, revealing a comparable sensitivity with commercial ultraviolet (UV) detectors. The compatibility of the proposed sensor to gradient elution is also demonstrated.

Index Terms—Degeneration mode, HPLC, microfluidic, microwave, modified square ring loaded resonator, isocratic and gradient elution.

## I. INTRODUCTION

TICROWAVE sensors, featured with low cost, labelfree detection and ease of integration, have been continuously developed for various microfluidic applications, such as measuring flow rate [1], [2] and cells in suspension [3]–[5], characterizing micro particles [6], [7] and liquid dielectric properties [8]-[11], monitoring bio-chemical concentrations [12]–[14] and gas/liquid quality [15], [16], and analyzing mixture compositions [17], [18]. But the development of microwave detectors, along with radiofrequency (RF) and refractive index (RI) detectors, for HPLC (High Performance Liquid Chromatography) gradient elution applications has been unsuccessful so far. Gradient elution is the main operation mode of HPLC, which is considered the third most used chemistry instrument. A major issue there is the carrier solution composition varies with time. Corresponding dielectric property variations overwhelm microwave as well as

Manuscript received July 21, 2020; accepted August 18, 2020. Date of publication August 21, 2020; date of current version December 16, 2020. This work was supported in part by the NSF under Grant 1711463. The associate editor coordinating the review of this article and approving it for publication was Dr. Sanket Goel. (Corresponding author: Pingshan Wang.)

The authors are with the Department of Electrical and Computer Engineering, Clemson University, Clemson, SC 29634 USA (e-mail: pwang@clemson.edu).

Digital Object Identifier 10.1109/JSEN.2020.3018683

RF and RI signals. In [19], we showed an interferometer-based microwave sensor which operated reasonably well under gradient HPLC elution conditions. The results show that microwave techniques are promising for universal HPLC detector applications and to address the issues associated with evaporative light scattering detectors (ELSDs), which are considered a universal method and more popular than mass spectroscopy. Nevertheless, the obtained microwave sensitivity, a 71.4 ppm LOD for caffeine detection, needs significant improvement for practical applications.

A simple microstrip transmission line (TL) was used in [19] with broadband operation capabilities similar to other TL-based dielectric spectroscopy sensors [20]-[23]. For high sensitivity, narrow-band resonators are well-known for concentrated electrical fields in the sensing zone and higher signal-to-noise ratio (SNR). Numerous resonator related work has been published. For instance, a novel microstrip split-ring resonator (SRR) with two gaps is proposed for measuring fluidic velocity and interrogating multiphase flow in [24]. However, the sensitivity is limited at high permittivity due to the depolarization effects. A whispering-gallery-mode resonator is designed in [25] for liquid complex permittivity measurement in nanoliter volumes. But the non-planar geometry limits the capability for lab-on-chip integration. A half-wavelength planar resonator integrated with an active feedback loop technique is proposed in [26] to boost the quality factor in the aquatic

1558-1748 © 2020 IEEE. Personal use is permitted, but republication/redistribution requires IEEE permission. See https://www.ieee.org/publications/rights/index.html for more information.

environment. Yet the sensitivity for microfluidic applications still needs to be demonstrated. The sensors in [27]–[30] are made of cavity resonators for the high-accuracy fluid profiling at microwave frequencies. Unfortunately, the complex design, modeling and construction are not desired.

Recently, some methods/techniques have been proposed to enhance the resonator sensitivity. A metamaterial-infused resonator is proposed in [31] to improve the coupling level, which results in enhanced sensitivity and linearity for high-permittivity liquids. In [18], a microwave sensor made of a transmission line loaded with parallel-connected series LC resonator is proposed. Just one capacitor is incorporated as sensing element in the resonant structure. Thus, the sensitivity can be improved without using distributed capacitors. In [32]–[34], a splitter/combiner configuration loaded with a pair of resonators is proposed to resist cross sensitivities caused by external factors, such as temperature and moisture variations. Some shape modifications in SRRs [35]–[38] are proposed to enhance the electrical field intensity for higher sensitivity.

In this work, we propose a dual-mode microwave microfluidic sensor based on a modified square ring loaded resonator (SRLR). The perturbation introduced by the liquidunder-test (LUT) results in separation of two degeneration modes, so that the resonant properties are fully exploited. By carefully tuning the gap size, the sensitivity for different permittivity ranges can be optimized and improved accordingly. The paper is arranged as the following. Section II describes the proposed resonator design, its equivalent circuit analysis and full-wave simulation verifications. Section III shows a microfluidic sensor based on the proposed resonator and the measurement results of water-methanol mixture. In addition, the sensor is connected in series with a commercial HPLC system for caffeine and sucrose detections under both isocratic and gradient elution. Section IV are discussions and conclusions.

## II. DUAL-MODE RESONATOR DESIGN

Figure 1 shows a schematic of the proposed sensor, in which a microstrip line and a rectangular ring are electrically shorted with a gap at the center. A microfluidic channel is placed above the gap. A vector network analyzer (VNA) is used for measurements. The introduction of LUT splits the degenerating resonance modes at  $f_1$  and  $f_2$ . The presence of analyte in flow will cause simultaneous  $f_1$  and  $f_2$  shifts in opposite directions, thus, contributing to sensor sensitivity enhancement.

## A. A Dual-Mode Ring-Based Resonator

Fig. 2 shows the equivalent circuit model of the proposed resonator with  $Z_i$  and  $\theta_i$ , the characteristic impedance and electrical length of corresponding TL sections in Fig. 1. The center gap can be modeled as a  $\pi$ -network of edge slot capacitances ( $C_{gap}$  and  $C_{end}$ ) [39], as shown in Fig. 2(a). Due to fringing field effects, both  $C_{gap}$  and  $C_{end}$  will be affected when LUT is introduced in the gap area. The values of  $C_{gap}$  and  $C_{end}$  will increase and decrease, respectively, along with increasing LUT permittivity ( $\varepsilon_{LUT}$ ). Under even-

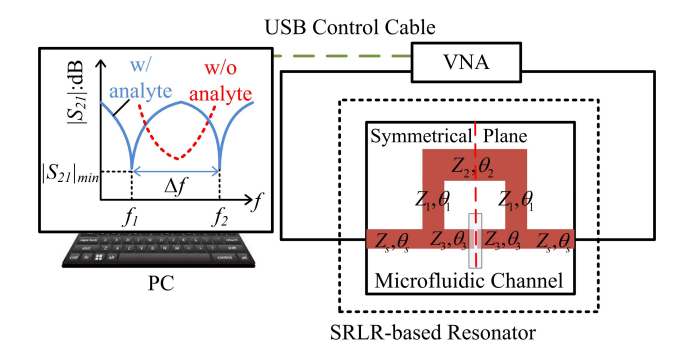


Fig. 1. The schematic of a dual-mode microwave microfluidic sensor based on a modified SRLR.

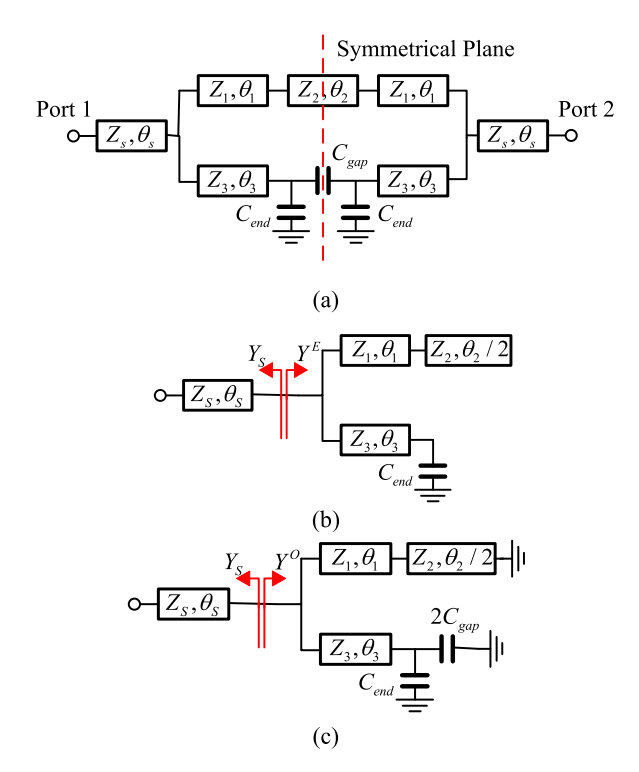


Fig. 2. (a) The equivalent circuit of the modified SRLR-based resonator. (b) Even-mode excitation equivalent circuit of the resonator. (c) Odd-mode excitation equivalent circuit of the resonator.

or odd-mode excitations, the symmetrical plane in Fig. 2(a) behaves as a perfect magnetic wall or a perfect electric wall, respectively. The bisection of the odd-mode and even-mode excitation equivalent circuit are in Fig. 2(b-c), where  $Y_S$  and  $Y^E/Y^O$  represent the corresponding input admittances from left and right sides of the bisection network under even-/odd-mode excitations. Based on even-odd analysis [40]–[42], the resonant condition for even-mode excitation in Fig. 2(b) can be derived as

$$Im(Y_S + Y^E) = 0 (1)$$

where

$$Y_S = \frac{Z_S + j Z_0 \tan \theta_S}{Z_S (Z_0 + j Z_S \tan \theta_S)}$$
 (2)

$$Y^{E} = -j \left[ \frac{1 + \frac{Z_{2}}{Z_{1}} \tan \theta_{1} \cot \frac{\theta_{2}}{2}}{Z_{1} \tan \theta_{1} - Z_{2} \cot \frac{\theta_{2}}{2}} + \frac{1 + \frac{1}{\omega C_{end} Z_{3}} \tan \theta_{3}}{Z_{3} \tan \theta_{3} - \frac{1}{\omega C_{end}}} \right]$$
(3)

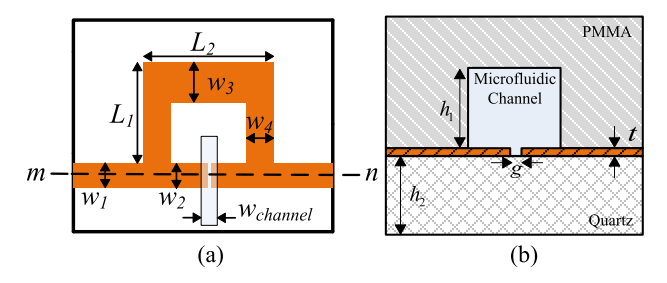


Fig. 3. (a) A top view of the proposed SRLR-based resonator layout for HFSS simulation and fabrication. (b) The cross section view along dash line *mn* in (a). The dimension of the resonator chip is 18mm×30mm.

 $Z_0$  is the system characteristic impedance, and  $\omega$  is radian frequency. Similarly, the resonant condition for odd-mode excitation in Fig. 2(c) can be written as

$$Im(Y_S + Y^O) = 0 (4)$$

where

$$Y^{O} = -j \left[ \frac{1 - \frac{Z_{2}}{Z_{1}} \tan \theta_{1} \tan \frac{\theta_{2}}{2}}{Z_{1} \tan \theta_{1} + Z_{2} \tan \frac{\theta_{2}}{2}} + \frac{1 + \frac{1}{\omega(2C_{gap} + C_{end})Z_{3}} \tan \theta_{3}}{Z_{3} \tan \theta_{3} - \frac{1}{\omega(2C_{gap} + C_{end})}} \right]$$
(5)

By substituting eq. (2) and (3) (or eq. (2) and (5)) into eq. (1) (or eq. (4)), the resonant frequency  $f_2$  (or  $f_1$ ) of even (or odd) modes can be determined. The multiple transmission line dimension parameters and the gap size provide the flexibility for design. The ratio of even- and odd-mode resonant frequency can be derived as

$$\frac{f_2}{f_1} \sim 1 + 2\frac{C_{gap}}{C_{end}} \tag{6}$$

which indicates larger resonant frequency separation when  $\varepsilon_{LUT}$  increases due to  $C_{gap}$  vs  $C_{end}$  ratio. Therein, the  $C_{gap}$  and  $C_{end}$  are both affected by the dielectric layers, indicating that the resonant modes, determined by eq. (1)-(5), can be indicators for dielectric property of LUTs. The two-frequency difference between the resonant modes, as shown in Fig. 1, is expressed as

$$f_d = |f_1 - f_2| \tag{7}$$

The sensitivity can be defined as [43]

$$S = \frac{\partial f_d}{\partial \varepsilon} = \frac{\Delta f_d}{\Delta \varepsilon} \tag{8}$$

where  $\Delta \varepsilon$  is LUT permittivity variation.

### B. Full-Wave Simulations

Full-wave simulations using *HFSS* (High Frequency Structure Simulator) are conducted for the SRLR-based resonator, shown in Fig. 3(a-b). The resonator dimensions are summarized in Table I. Four resonators with different gap size from 10  $\mu$ m to 90  $\mu$ m are simulated while sweeping the LUT permittivity from 1 to 80 with a constant tangent loss of 0.055.

Fig. 4 shows LUT permittivity effects on resonant modes when the gap size is 90  $\mu$ m. It's noteworthy that the two

TABLE I
PARAMETERS OF THE SRLR-BASED RESONATOR

Parameter	Symbol	Value
Metal layer Thickness	t	240 <i>n</i> m
Gap Size	g	$10/30/50/90 \mu m$
Channel Height	$h_I$	$250  \mu \mathrm{m}$
Channel Width	$W_{channel}$	$250  \mu \mathrm{m}$
Channel Relative Permittivity (PMMA)	$\mathcal{E}_{channel}$	3.4 <i>-j</i> 0.0034
LUT Relative Permittivity	$arepsilon_{LUT}$	unknown
Substrate Thickness (Quartz)	$h_2$	1 mm
Substrate Relative Permittivity	$\mathcal{E}_{sub}$	3.78
Resonator Dimension	$w_I$	2.2 mm
	$w_2$	2.2 mm
	$w_3$	3 mm
	$W_4$	2.5 mm
	$L_I$	8.7 mm
	$L_2$	9 mm

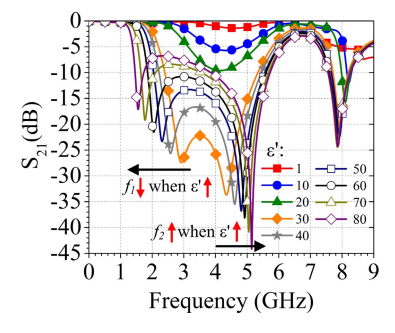


Fig. 4. Demonstration of LUT permittivity effects on the degeneration modes when the gap size is 90  $\mu$ m. The tangent loss (tan $\delta$ ) of LUT is always 0.055.

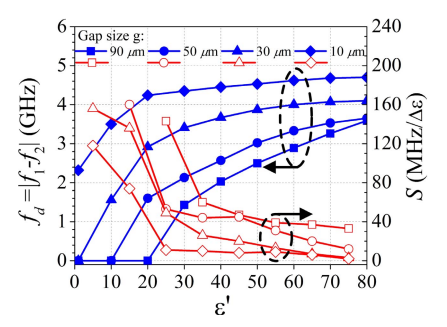


Fig. 5. Frequency distance between the two degeneration modes and sensitivity for different gap sizes from 10  $\mu$ m to 90  $\mu$ m.

degeneration modes don't split until the LUT permittivity is larger than 20. When the permittivity increases from 30 to 80,  $f_1$  decreases while the  $f_2$  increases, resulting an increasing frequency difference  $\Delta f$ . Fig. 5 shows  $\Delta f$  vs. LUT permittivity for different gap sizes from 10  $\mu$ m to 90  $\mu$ m, as well as the corresponding sensitivity. It is shown that all the simulated nonlinear curves have an  $\varepsilon$ ' threshold value, after which there is a sharp  $\Delta f$  slope, indicating a high sensitivity. The sensitivity gradually decreases along the increasing  $\varepsilon$ '. The "threshold" permittivity is determined by the gap size, which determines at what  $\varepsilon$ ' the two degeneration modes start to split. These features enable the proposed resonator to be optimized for various applications for different dielectric liquids. It's noteworthy that under gradient elution in HPLC applications, the analytes usually elute out by low water-volume mobile

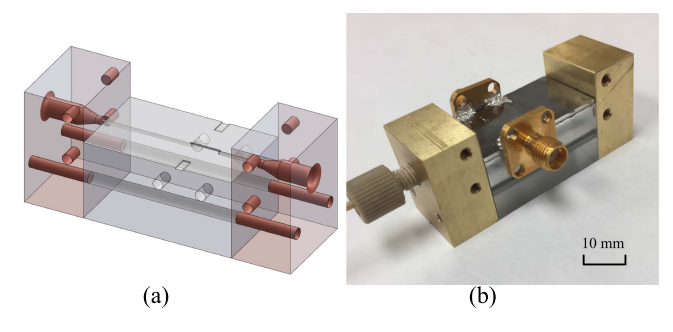


Fig. 6. (a) Microfludic channel parts for holding the resonator chip and connecting to HPLC system. (b) A picture of the assembled sensor.

phase, i.e. low-permittivity solution. Therefore, the capability to sustain high sensitivity performance under low permittivity makes this design a promising sensor for minute sample detection under gradient elution.

# III. EXPERIMENTAL MEASUREMENTS

The sensors with gap size of 10  $\mu$ m, 30  $\mu$ m and 90  $\mu$ m, are built to verify the proposed sensor. The resonators are fabricated with standard microfabrication techniques on a 1-mmthick quartz wafer. A 200-nm-thick copper film is deposited on a 20-nm-thick Ti adhesion layer to form the resonator structure. Another 20-nm-thick Ti is deposited on the copper layer. The dimensions of the loaded ring structure are listed in Table I. The microfluidic channel, shown in Fig. 6 (a), is made with Polymethyl methacrylate (PMMA). A 250  $\mu$ m wide and 250  $\mu$ m deep trench is mechanically milled and aligned with the gap area. Then, the resonator chip is bonded to the PMMA microfluidic channel with ultraviolet (UV) glue, as shown in Fig. 6(b). The female tapered fittings drilled in the metal parts allow an easy connection to the HPLC system. A vector network analyzer (VNA) operating from 100 KHz to 8 GHz is used to measure the S parameters.

## A. Water-Methanol Mixtures Measurements

Some water-methanol mixtures with water volume fractions from 0% to 100% are prepared to characterize sensors' broadband performance. Corresponding to the increasing water volume fraction, the calculated  $\varepsilon$ ' increases from 27 to 78 [44]. A programmable single syringe pumps (NE-1010) is used to fill the liquids in the microfluidic channel. Fig. 7 shows the measured broadband S<sub>21</sub> performance of the sensor with a 90-µm gap for these water-methanol mixtures. The shifts of resonating frequencies  $(f_1, f_2)$  agrees well with the simulated results in Fig. 4. Similarly, the sensors with gaps of 10  $\mu$ m and 30  $\mu$ m are also measured, and the frequency differences ( $\Delta f = f_2 - f_1$ ) and sensitivity are plotted in Fig. 8. For the sensor with a  $90-\mu m$ gap, the sensitivity at 40% water-methanol is estimated as 50 MHz/ $\Delta \varepsilon$ '. Table II summarizes the performance of some published resonator-based sensors. It shows that our proposed sensor has high sensitivity.

#### B. HPLC Measurements

Caffeine and sucrose in DI-water solutions are prepared with different concentrations for HPLC measurements. The sensor

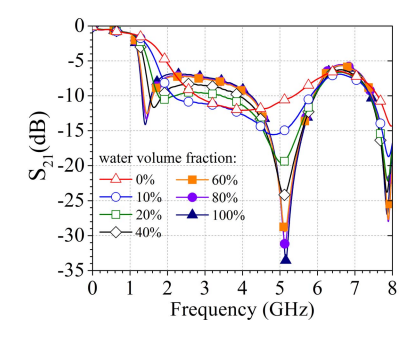


Fig. 7. The measured  $S_{21}$  of the sensor with a 90- $\mu$ m gap for various water-methanol mixtures from 100 KHz to 8GHz. The water volume fraction varies from 0% to 100%.

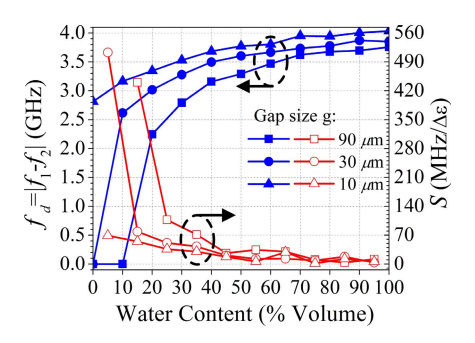


Fig. 8. Measured frequency distance between the two degeneration modes and sensitivity for different sensors with gap sizes of 10  $\mu$ m, 30  $\mu$ m and 90  $\mu$ m.

TABLE II

COMPARISON OF THE RESONATING-BASED MICROFLUDIC SENSORS

Ref.	Sensitivity	Resonating Frequency	Q factor (sample)	Volume	Year
[45]	5.28 MHz/Δε'	2.1 GHz	27 (water)	462 nL	2014
[46]	0.57 MHz/Δε'	5.85 GHz	191	Immersed	2015
			(water)	in solution	
[47]	5.25 MHz/Δε'	2 GHz	525 (air)	61 nL	2017
[16]	0.66 MHz/Δε'	2.3 GHz	47 (water)	589 <i>n</i> L	2018
[48]	14.25 MHz/Δε'	2.1 GHz	48 (air)	$2 \mu L$	2019
[18]	8.7 MHz/Δε'	1.91 GHz	26 (water)	390 nL	2019
This	90- $\mu$ m gap:	$f_l$ =1.4 GHz	$Q_1 = 46.9$	137.5 nL	2020
work	50 MHz/Δε'	$f_2$ =5.16 GHz	$Q_2 = 26.4$		
	at 40% water-	-	(water)		
	methanol				

system, as illustrated in Fig. 1, is connected in series with the reverse HPLC-UV system Ultimate 3000, which consists of a pump system, an auto-sampler, a column compartment and a various wavelength UV detector from Thermo Fisher Scientific. Eluents are separated by an EVO C<sub>18</sub> column  $(4.6 \times 250 \text{ mm}, 5 \mu\text{m} \text{ particle}, \text{Kiretex}, \text{North America}).$ HPLC-grade methanol and DI water are used as mobile phase A and B, respectively. For caffeine and sucrose detection measurements, the isocratic elution is performed at a ratio of 60:40 or 40:60 (A:B) while the gradient elution starts from 15:85 (A:B), reached 85:15 and then goes back to 15:85. The injection volume is 100  $\mu$ L. Table III summarizes the mobile phase programs. For HPLC measurement of minute analyte in carrier solution, the single resonating-frequency monitoring method [49] is used for a high data-acquisition rate and low noise performance. The first odd-mode resonating frequency

TABLE III
HPLC ELUTION PROGRAM

Mobile Phase	Analyte	Elution Mode	Flow Rate	Time	A:B
	Caffeine	Isocratic	0.2 mL/min	20 min	60:40
	Sucrose	Isocratic	0.6 mL/min	10 min	40:60
Methanol (A)	Caffeine	Gradient	0.2 mL/min	0 min	15:85
DI water (B)				6 min	50:50
				12 min	85:15
				18 min	50:50
				24 min	15:85

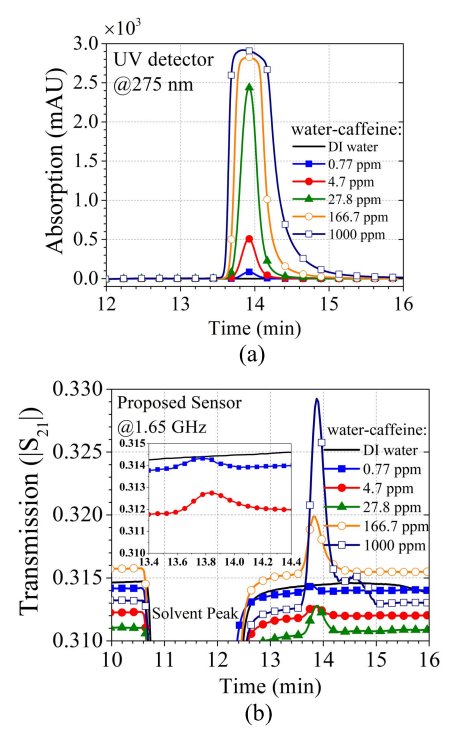


Fig. 9. The measured responses of (a) UV detector and (b) the proposed sensor for water-caffeine samples from 0.77 ppm to 1000 ppm. The inset in (b) zooms in the signal peak from 13.4 to 14.4 min for DI water, 0.77 ppm and 4.7 ppm water-caffeine samples.

 $f_1$  is selected due to the stronger interaction between the electrical field and analytes when compared to the even-mode one. The sensor with the 10- $\mu$ m gap is selected for demonstration. A data-acquisition rate of 20 Hz is achieved.

To examine the sensitivity of the sensor, the water-caffeine samples with concentrations from 0.77 ppm to 1000 ppm are measured under isocratic elution. Figure 9 shows the measured responses of the commercial UV detector and the proposed sensor, respectively, where the retention time of caffeine is at  $\sim$ 13.9 min. The solvent of analytes that will not be trapped by the column is eluted out firstly at  $\sim$  11.2 min. The parameters of fitting polynomial regression curve for signal heights are summarized in Table IV. The correlation coefficients  $R^2$  for the polynomial regression line is 0.9874, indicating a good agreement to the measured one. Besides, the limit of detection (LOD) for caffeine can be estimated by considering an SNR of 3. The estimated LOD of the sensor on caffeine is 0.231 ppm. According to the injection volume, the minimum detectable quantity (MDQ) is calculated

TABLE IV
SENSITIVITY OF THE PROPOSED MICROWAVE SENSOR
MEASUREMENTS ON WATER-CAFFEINE

Concentration (x: ppm)	0	0.77	4.7	27.8	166.7	1000
Signal Height (Δ S <sub>21</sub>  )	0	0.0004	0.001	0.0024	0.0048	0.0166
Polynomial Regression	$\Delta  S_{21}  = 0.0004x^3 - 0.0034x^2 + 0.0084x - 0.0057$					
$R^2$	0.9874					
Noise $(\Delta   S_{21}  )$	0.0	00004				
LOD (ppm)	0.231					
MDQ (ng)	23	.1				

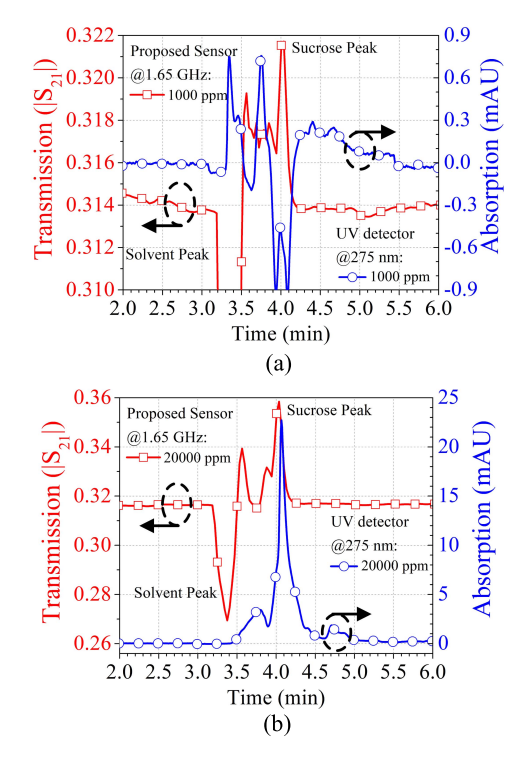


Fig. 10. The proposed sensor detection of (a) 1000 ppm and (b) 20000 ppm water-sucrose samples under isocratic elution. UV detector result is included for comparison.

to be 23.1 ng. When compared to the UV detector results, where the LOD is estimated to be 0.03 ppm, the proposed sensor is ~8 times less sensitive. In addition, Fig. 10 shows the measured results of water-sucrose at the concentration of 1000 ppm and 20000 ppm, respectively. The solvent and caffeine are eluted at ~3.4min and ~4 min, respectively. The signal peak of 1000 ppm water-sucrose in the UV detector is overwhelmed by the noise while being clearly detected in the proposed microwave sensor. The proposed sensor demonstrates a higher sensitivity than the UV detector on sucrose detection. For the analytes that lack strong chromophores of UV absorption, the proposed sensor can be used as an alternative universal detection technique, and it demonstrates a superior sensitivity than ELSD and RI detectors [50].

To verify the gradient-elution repeatability of the proposed sensor, three gradient elution tests with 100  $\mu$ L blank injection (DI water) are performed at 1.65 GHz. The gradient elution program is provided in Table III. Figure 11 shows that the results are highly reproducible with indistinguishable deviations. The relative standard

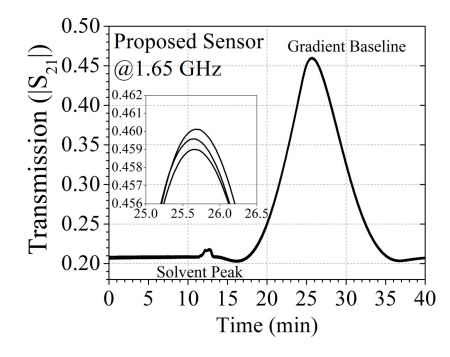


Fig. 11. Repeatability tests under gradient elution with a 100  $\mu$ L DI water injection. The deviations between the tests are within the line thickness. The inset zooms in the gradient baseline between 25 min and 26.5 min.

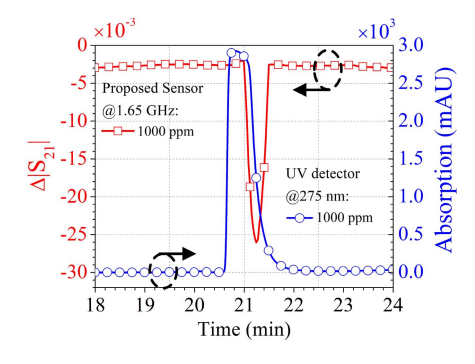


Fig. 12. The proposed sensor detection of 1000 ppm water-caffeine sample under gradient elution by subtracting the results of DI-water injection. UV detector result is included for comparison.

deviation (RSD) of gradient peak height and area is within 0.38% and 0.15%, respectively. Then a 100  $\mu$ L aliquot of 1000 ppm water-caffeine is injected and measured under the same condition. Since the signal of the caffeine sample is orders of magnitude smaller than gradient baseline, the curves with blank injection are subtracted from the ones with caffeine injection. Then the signal of caffeine sample is clearly obtained in Figure 12, which shows that the developed microwave sensor functions properly under gradient HPLC elution. The signal height is 0.0232. It's noteworthy that the SNR is deteriorated when compared to the isocratic case. It's mainly caused by larger baseline noise.

## IV. DISCUSSION AND CONCLUSION

The proposed resonator is shown to achieve a high sensitivity over a wide LUT permittivity range. Similar to the optical microring resonator arrays proposed in [51], the wide detection dynamic range allows microwave SRLR sensor to work under gradient elution. The sensitivities on caffeine detection under gradient elution are comparable to that of RI detectors under isocratic elution.

Based on a square ring loaded resonator, a microwave sensor technique is proposed and investigated for HPLC detector applications. Two resonating modes are both affected by the loaded LUT. The sensitivity for different dielectric liquids can be optimized by tuning the gap size of the ring. In static-flow measurements of water-methanol mixtures at different volume fractions, the proposed sensor achieves a sensitivity of 50 MHz/ $\Delta \varepsilon$ ' at 40% water-methanol when the distance

between two resonating modes is used as signal indicator. When connected to a commercial HPLC system under isocratic elution, the water-caffeine samples from 0.77 ppm to 1000 ppm are successfully detected by monitoring at a single frequency. Besides, the water-sucrose samples at 1000 ppm and 20000 ppm, whose signals are weak in UV detector, are measured with the proposed sensor. Under gradient elution, the water-caffeine at 1000 ppm is successfully detected with a higher signal peak while smaller SNR than that under isocratic elution. In conclusion, a sensitive microwave sensor that is compatible with HPLC gradient elution is achieved. It's a promising technique as an alternative universal detector for HPLC applications.

#### **ACKNOWLEDGMENT**

The authors gratefully acknowledge D. Lipscomb at L. G. Rich Environmental Research Laboratory for maintaining HPLC system and preparing analytes, and L. Wang, Dr. K. Marcus at Department of Chemistry for HPLC preliminary tests.

#### REFERENCES

- A. Penirschke, M. Schußler, and R. Jakoby, "New microwave flow sensor based on a left-handed transmission line resonator," in *IEEE MTT-S Int. Microw. Symp. Dig.*, Jun. 2007, pp. 393–396.
- [2] M. H. Zarifi, H. Sadabadi, S. H. Hejazi, M. Daneshmand, and A. Sanati-Nezhad, "Noncontact and nonintrusive microwavemicrofluidic flow sensor for energy and biomedical engineering," *Sci. Rep.*, vol. 8, no. 1, p. 139, Dec. 2018.
- [3] Y. Yang et al., "Distinguishing the viability of a single yeast cell with an ultra-sensitive radio frequency sensor," Lab a Chip, vol. 10, pp. 553–555, Jan. 2010.
- [4] N. M. N. Haase, G. Fuge, H. K. Trieu, A.-P. Zeng, and A. F. Jacob, "Miniaturized transmission-line sensor for broadband dielectric characterization of biological liquids and cell suspensions," *IEEE Trans. Microw. Theory Techn.*, vol. 63, no. 10, pp. 3026–3033, Oct. 2015.
- [5] A. Tamra, D. Dubuc, M.-P. Rols, and K. Grenier, "Microwave monitoring of single cell monocytes subjected to electroporation," *IEEE Trans. Microw. Theory Techn.*, vol. 65, no. 9, pp. 3512–3518, Sep. 2017.
- [6] J. Leroy et al., "Microfluidic biosensors for microwave dielectric spectroscopy," Sens. Actuators A, Phys., vol. 229, pp. 172–181, Jun. 2015.
- [7] T.-T. Tsai et al., "High throughout and label-free particle sensor based on microwave resonators," Sens. Actuators A, Phys., vol. 285, pp. 652–658, Jan. 2019.
- [8] W. Withayachumnankul, K. Jaruwongrungsee, A. Tuantranont, C. Fumeaux, and D. Abbott, "Metamaterial-based microfluidic sensor for dielectric characterization," *Sens. Actuators A, Phys.*, vol. 189, pp. 233–237, Jan. 2013.
- [9] E. L. Chuma, Y. Iano, G. Fontgalland, and L. L. Bravo Roger, "Microwave sensor for liquid dielectric characterization based on metamaterial complementary split ring resonator," *IEEE Sensors J.*, vol. 18, no. 24, pp. 9978–9983, Dec. 2018.
- [10] C.-S. Lee, B. Bai, Q.-R. Song, Z.-Q. Wang, and G.-F. Li, "Open complementary split-ring resonator sensor for dropping-based liquid dielectric characterization," *IEEE Sensors J.*, vol. 19, no. 24, pp. 11880–11890, Dec. 2019.
- [11] A. Ebrahimi, J. Scott, and K. Ghorbani, "Ultrahigh-sensitivity microwave sensor for microfluidic complex permittivity measurement," *IEEE Trans. Microw. Theory Techn.*, vol. 67, no. 10, pp. 4269–4277, Oct. 2019.
- [12] K. K. Adhikari and N.-Y. Kim, "Ultrahigh-sensitivity mediator-free biosensor based on a microfabricated microwave resonator for the detection of micromolar glucose concentrations," *IEEE Trans. Microw. Theory Techn.*, vol. 64, no. 1, pp. 319–327, Jan. 2016.
- [13] R. Narang et al., "Sensitive, real-time and non-intrusive detection of concentration and growth of pathogenic bacteria using microfluidicmicrowave ring resonator biosensor," Sci. Rep., vol. 8, no. 1, p. 15807, Oct. 2018.
- [14] G. Govind and M. J. Akhtar, "Metamaterial-inspired microwave microfluidic sensor for glucose monitoring in aqueous solutions," *IEEE Sensors J.*, vol. 19, no. 24, pp. 11900–11907, Dec. 2019.

- [15] M. Abou-Khousa, A. Al-Durra, and K. Al-Wahedi, "Microwave sensing system for real-time monitoring of solid contaminants in gas flows," *IEEE Sensors J.*, vol. 15, no. 9, pp. 5296–5302, Sep. 2015.
- [16] S. Mohammadi, A. V. Nadaraja, D. J. Roberts, and M. H. Zarifi, "Real-time and hazard-free water quality monitoring based on microwave planar resonator sensor," *Sens. Actuators A, Phys.*, vol. 303, pp. 111663–111674, Mar. 2020.
- [17] D. J. Rowe, A. Porch, D. A. Barrow, and C. J. Allender, "Microfluidic device for compositional analysis of solvent systems at microwave frequencies," Sens. Actuators B, Chem., vol. 169, pp. 213–221, Jul. 2012.
- [18] Y. Cui and P. Wang, "The design and operation of ultra-sensitive and tunable radio-frequency interferometers," *IEEE Trans. Microw. Theory Techn.*, vol. 62, no. 12, pp. 3172–3182, Dec. 2014.
- [19] D. Ye, W. Wang, D. Moline, M. S. Islam, F. Chen, and P. Wang, "A microwave flow detector for gradient elution liquid chromatography," *Anal. Chem.*, vol. 89, no. 20, pp. 10761–10768, Oct. 2017.
- [20] K. Grenier et al., "Integrated broadband microwave and microfluidic sensor dedicated to bioengineering," IEEE Trans. Microw. Theory Techn., vol. 57, no. 12, pp. 3246–3253, Dec. 2009.
- [21] J. C. Booth, N. D. Orloff, J. Mateu, M. Janezic, M. Rinehart, and J. A. Beall, "Quantitative permittivity measurements of nanoliter liquid volumes in microfluidic channels to 40 GHz," *IEEE Trans. Instrum. Meas.*, vol. 59, no. 12, pp. 3279–3288, Dec. 2010.
- [22] S. Liu et al., "Hybrid characterization of nanolitre dielectric fluids in a single microfluidic channel up to 110 GHz," *IEEE Trans. Microw. Theory Techn.*, vol. 65, no. 12, pp. 5063–5073, Dec. 2017.
- [23] D. Ye, M. S. Islam, G. Yu, and P. Wang, "A single-line single-channel method with closed-form formulas for the characterization of dielectric liquids," *IEEE Trans. Microw. Theory Techn.*, vol. 67, no. 6, pp. 2443–2450, Jun. 2019.
- [24] A. A. Abduljabar, D. J. Rowe, A. Porch, and D. A. Barrow, "Novel microwave microfluidic sensor using a microstrip split-ring resonator," *IEEE Trans. Microw. Theory Techn.*, vol. 62, no. 3, pp. 679–688, Mar. 2014.
- [25] A. I. Gubin et al., "Whispering-gallery-mode resonator technique with microfluidic channel for permittivity measurement of liquids," *IEEE Trans. Microw. Theory Techn.*, vol. 63, no. 6, pp. 2003–2009, Jun. 2015.
- [26] M. H. Zarifi and M. Daneshmand, "Liquid sensing in aquatic environment using high quality planar microwave resonator," Sens. Actuators B, Chem., vol. 225, pp. 517–521, Mar. 2016.
- [27] G. Gennarelli, S. Romeo, M. R. Scarfi, and F. Soldovieri, "A microwave resonant sensor for concentration measurements of liquid solutions," *IEEE Sensors J.*, vol. 13, no. 5, pp. 1857–1864, May 2013.
- [28] A. H. Sklavounos and N. S. Barker, "Liquid-permittivity measurements using a rigorously modeled overmoded cavity resonator," *IEEE Trans. Microw. Theory Techn.*, vol. 62, no. 6, pp. 1363–1372, Jun. 2014.
- [29] M. B. Barmatz, H. W. Jackson, A. S. Javeed, C. S. Jamieson, and D. E. Steinfeld, "An accurate radially stratified approach for determining the complex permittivity of liquids in a cylindrical microwave cavity," *IEEE Trans. Microw. Theory Techn.*, vol. 63, no. 2, pp. 504–508, Feb. 2015.
- [30] Z. Wei et al., "A high-sensitivity microfluidic sensor based on a substrate integrated waveguide re-entrant cavity for complex permittivity measurement of liquids," Sensors, vol. 18, no. 11, p. 4005, Nov. 2018.
- [31] M. Abdolrazzaghi, M. Daneshmand, and A. K. Iyer, "Strongly enhanced sensitivity in planar microwave sensors based on metamaterial coupling," *IEEE Trans. Microw. Theory Techn.*, vol. 66, no. 4, pp. 1843–1855, Apr. 2018.
- [32] L. Su, J. Mata-Contreras, P. Vélez, and F. Martín, "Splitter/combiner microstrip sections loaded with pairs of complementary split ring resonators (CSRRs): Modeling and optimization for differential sensing applications," *IEEE Trans. Microw. Theory Techn.*, vol. 64, no. 12, pp. 4362–4370, Dec. 2016.
- [33] J. Naqui et al., "Transmission lines loaded with pairs of stepped impedance resonators: Modeling and application to differential permittivity measurements," *IEEE Trans. Microw. Theory Techn.*, vol. 64, no. 11, pp. 3864–3877, Nov. 2016.
- [34] A. Ebrahimi, G. Beziuk, J. Scott, and K. Ghorbani, "Microwave differential frequency splitting sensor using magnetic-LC resonators," *Sensors*, vol. 20, no. 4, p. 1066, Feb. 2020.
- [35] X.-J. He, Y. Wang, J.-M. Wang, and T.-L. Gui, "Thin-film sensor based tip-shaped split ring resonator metamaterial for microwave application," *Microsyst. Technol.*, vol. 16, no. 10, pp. 1735–1739, Oct. 2010.
- [36] A. K. Horestani, C. Fumeaux, S. F. Al-Sarawi, and D. Abbott, "Split ring resonators with tapered strip width for wider bandwidth and enhanced resonance," *IEEE Microw. Wireless Compon. Lett.*, vol. 22, no. 9, pp. 450–452, Sep. 2012.

- [37] D. J. Rowe, S. Al-Malki, A. A. Abduljabar, A. Porch, D. A. Barrow, and C. J. Allender, "Improved split-ring resonator for microfluidic sensing," *IEEE Trans. Microw. Theory Techn.*, vol. 62, no. 3, pp. 689–699, Mar. 2014.
- [38] A. Ebrahimi, J. Scott, and K. Ghorbani, "Microwave reflective biosensor for glucose level detection in aqueous solutions," *Sens. Actuators A*, *Phys.*, vol. 301, Jan. 2020, Art. no. 111662.
- [39] M. Maeda, "An analysis of gap in microstrip transmission lines," IEEE Trans. Microw. Theory Techn., vol. MTT-20, no. 6, pp. 390–396, Jun. 1972.
- [40] S. Luo, L. Zhu, and S. Sun, "A dual-band ring-resonator bandpass filter based on two pairs of degenerate modes," *IEEE Trans. Microw. Theory Techn.*, vol. 58, no. 12, pp. 3427–3432, Dec. 2010.
- [41] S. Sun, "A dual-band bandpass filter using a single dual-mode ring resonator," *IEEE Microw. Wireless Compon. Lett.*, vol. 21, no. 6, pp. 298–300, Jun. 2011.
- [42] H. Liu, B. Ren, X. Guan, P. Wen, and Y. Wang, "Quad-band high-temperature superconducting bandpass filter using quadruple-mode square ring loaded resonator," *IEEE Trans. Microw. Theory Techn.*, vol. 62, no. 12, pp. 2931–2941, Dec. 2014.
- [43] A. Ebrahimi, J. Scott, and K. Ghorbani, "Differential sensors using microstrip lines loaded with two split-ring resonators," *IEEE Sensors J.*, vol. 18, no. 14, pp. 5786–5793, Jul. 2018.
- [44] T. Sato, A. Chiba, and R. Nozaki, "Hydrophobic hydration and molecular association in methanol-water mixtures studied by microwave dielectric analysis," *J. Chem. Phys.*, vol. 112, no. 6, pp. 2924–2932, Feb. 2000.
- [45] A. Ebrahimi, W. Withayachumnankul, S. Al-Sarawi, and D. Abbott, "High-sensitivity metamaterial-inspired sensor for microfluidic dielectric characterization," *IEEE Sensors J.*, vol. 14, no. 5, pp. 1345–1351, May 2014.
- [46] C. Liu and F. Tong, "An SIW resonator sensor for liquid permittivity measurements at C band," *IEEE Microw. Wireless Compon. Lett.*, vol. 25, no. 11, pp. 751–753, Nov. 2015.
- [47] A. A. M. Bahar, Z. Zakaria, S. R. A. Rashid, A. A. M. Isa, and A. R. Alahnomi, "Dielectric analysis of liquid solvents using microwave resonator sensor for high efficiency measurement," *Microw. Opt. Techn. Lett.*, vol. 59, no. 2, pp. 2781–2784, Feb. 2017.
- [48] X. Zhang, C. Ruan, T. Haq, and K. Chen, "High-sensitivity microwave sensor for liquid characterization using a complementary circular spiral resonator," *Sensors*, vol. 19, no. 4, p. 787, Feb. 2019.
- [49] Y. Cui, W. F. Delaney, T. Darroudi, and P. Wang, "Microwave measurement of giant unilamellar vesicles in aqueous solution," *Sci. Rep.*, vol. 8, no. 1, pp. 1–8, Dec. 2018.
- [50] M. Swartz, "HPLC detectors: A brief review," J. Liquid Chromatogr. Rel. Technol., vol. 33, nos. 9–12, pp. 1130–1150, Jul. 2010.
- [51] J. H. Wade and R. C. Bailey, "Refractive index-based detection of gradient elution liquid chromatography using chip-integrated microring resonator arrays," *Anal. Chem.*, vol. 86, no. 1, pp. 913–919, Jan. 2014.

**Duye Ye** received the B.Eng. and M.Eng. degrees from the Beijing University of Posts and Telecommunications, Beijing, China, in 2012 and 2015, respectively. He is currently pursuing the Ph.D. degree in electrical and electronic engineering with Clemson University, SC, USA. His research interests include RF/microwave sensors design for biomedical applications and RF circuits design for communication systems.

Omkar received the bachelor's degree with a major in electronics and communication engineering and a minor in mathematics from Shiv Nadar University, Greater Noida, India. He is currently pursuing the master's degree with Clemson University, SC, USA. His research interests include electromagnetics for biomedical applications, and antennas and integrated circuits design for wireless devices and systems.

Pingshan Wang (Senior Member, IEEE) received the Ph.D. degree in electrical and computer engineering from Cornell University, Ithaca, NY, USA, in 2004. He is currently a Professor with the Department of Electrical and Computer Engineering, Clemson University, Clemson, SC, USA. His current research is on developing high-frequency lab-on-achip techniques, for which he and his group develop electronic devices, circuits, and systems at microwave and millimeter frequencies. They also develop high-frequency microfluidic and nanofluidic devices and study the high-frequency properties of biological and chemical substances.